AIAA JOURNAL
Vol. 42, No. 7, July 2004

Identification of Viscoelastic Fractional Complex Modulus

T. Beda*
Polytechnic National Advanced School, Yaounde, Cameroon
and
Y. Chevalier†
Institut Supérieur des Matériaux et de la Construction Mécanique, 93407 Saint-Ouen Cedex, France

An examination is made of a graphical method and derived techniques to characterize the fractional complex modulus of simple and complex viscoelastic materials, by a fit of experimental data, as well as from all of the various states of a material, that is, rubbery, transition, and glassy regions, rather than from that limited just to the sole transition domain, a situation that often occurs in materials investigation. Concrete results of some useful materials are illustrated.

Nomenclature

D^β	=	fractional derivative of order β
E_{inf}	=	inflexion magnitude
$E(\omega)$	=	magnitude of complex modulus
E_0	=	static Young's modulus
$E^*(\omega)$	=	complex modulus
$E'(\omega)$	=	real part of complex modulus
$E''(\omega)$	=	imaginary part of complex modulus
j^2	=	-1
s	=	Laplace variable
t	=	time
z_1, z_2	=	complex numbers (model parameters)
α, β, a, b, c	=	model parameters (real numbers)
Γ	=	gamma function
$\varepsilon(t)$	=	strain
$\varepsilon^*(\omega)$	=	Fourier transform of $\varepsilon(t)$
$\eta_{\max}$	=	maximum loss factor
$\eta(\omega)$	=	loss factor
κ	=	damping ratio
$\sigma(t)$	=	stress
$\sigma^*(\omega)$	=	Fourier transform of $\sigma(t)$
τ, τ_0, τ_1	=	time constants
ω	=	frequency
$\omega_c, \omega_0, \omega_1$	=	cutoff frequencies
ω_f	=	fixed frequency
ω_{inf}	=	inflexion frequency
ω_n	=	undamped natural frequency

I. Introduction

VISCOELASTIC damping is becoming widely used for vibration and noise control in aerospace, automotive engineering, and propulsion. Its description by fractional derivatives is becoming more attractive in structures calculus. Interest in this approach lies in that the mathematical model renders optimum the number of empirical parameters required to define the frequency-dependent mechanical properties. Bagley and Torvik,[1] Koeller,[2] and Rogers[3] have contributed greatly to the use of fractional calculus to construct stress–strain relationships for viscoelastic materials. Fractional calculus has been established as the basis for an accurate and efficient model for complex modulus.

Difficulties that this model presents come from the identification of relative empirical parameters, some of which are fractional power factors. The usual methods preestablish the power-factors' values to simplify the problem considerably because their evaluation becomes irrelevant and the parameters sought are reduced. The Bode diagram method is not recommended for high damping materials, however, because it requires evaluation of too many parameters,[4] which is a source of errors. Even for methods that settle a priori the fractional power factors that are inspired by Bode diagram methods, the number of parameters remains high.[3,5] On the other hand, the usual nonlinear numerical methods, which are all iterative identification procedures, require the user to have a great deal of experience. Recently, Jones[6] reviewed the analysis of test data for evaluating the quality of available complex modulus data. Accurate and efficient identification procedures have been aided by the use of the Wicket plot and statistical methods. These are not the usual definitions of mean square errors because it is the use of logarithms in the error definitions that are not normalized with the number of data points. Although good results have been obtained, the use of these procedures requires the user to master the statistical process: good choice of initial values, stability of error minimization, local minima recognition, etc. Therefore analysis should be carried out very carefully.

This contribution is an attempt to render simpler the identification of simple and complex fractional models by a graphical method and some derived procedures.

II. Viscoelastic Complex Modulus

A. Simple Viscoelastic Fractional Model

For many thermorheologically simple and macroscopically homogenous viscoelastic materials, including a large family of macromolecular, thermostiffening and thermoplastic materials and elastomers, the constitutive equation for linear behavior can be defined by a simple model given by[1]

$$\sigma(t) + aD^\alpha\langle\sigma(t)\rangle = E_0\varepsilon(t) + bD^\alpha\langle\varepsilon(t)\rangle \qquad (1)$$

where

$$D^\alpha\langle f(t)\rangle = \frac{1}{\Gamma(1-\alpha)}\frac{\mathrm{d}}{\mathrm{d}t}\int_0^t \frac{f(\xi)}{(t-\xi)^\alpha}\,\mathrm{d}\xi, \qquad 0 < \alpha < 1 \qquad (2)$$

In the Laplace–Carson transform domain, taking the Fourier transform of Eq. (1), one obtains

$$[1 + a(j\omega)^\alpha]\sigma^*(\omega) = \left[E_0 + b(j\omega)^\alpha\right]\varepsilon^*(\omega) \qquad (3)$$

Equation (3) can be rewritten as

$$\sigma^*(\omega) = E^*(\omega)\varepsilon^*(\omega) \qquad (4)$$

Received 19 January 2002; revision received 3 August 2003; accepted for publication 18 October 2003.

*Professor, Department of Industrial and Mechanical Engineering, University of Yaounde I, B.P. 8390.

†Professor, Laboratoire d'Ingénierie Intégré des Systèmes Mécaniques et des Matériaux, Rheology and Structures Group, Paris; tbeda@polytech.uninet.cm.

$E^*(\omega)$ is the complex Young's modulus. It can be expressed as

$$E^*(\omega) = E_0 \frac{1+\left[j(\omega/\omega_0)^\alpha\right]}{1+\left[j(\omega/\omega_1)^\alpha\right]} \tag{5}$$

or

$$E^*(\omega) = E_0 \frac{1+(j\tau_0\omega)^\alpha}{1+(j\tau_1\omega)^\alpha} \tag{6}$$

The complex modulus is, therefore, a function of the frequency to the power of a fractional number. For the multiform function $(j\omega)^\alpha$, where α is a fractional number less than one, we take part of the principal resolution $(0 \le \theta \le 2\pi)$ because of the relaxation function property.[4]

For such a material, the linear viscoelastic behavior is completely defined by four mechanical parameters, E_0, ω_0, ω_1, and α characteristics of the material, where the material is simple.

The focus is first on an evaluation of these parameters from experimental gain or/and complex data given over a range of frequencies.

B. Mechanical Properties

1. Magnitude Function

Given $E(\omega) = |E^*(\omega)|$, the magnitude of $E^*(\omega)$, from relation (6), one has

$$\log E(\omega) = \log E_0 + \log\left|1+(j\tau_0\omega)^\alpha\right| - \log\left|1+(j\tau_1\omega)^\alpha\right| \tag{7}$$

For the inflexion point of the magnitude function,

$$\log E(\omega) = \log E_0 + \tfrac{1}{2}\log\left[1+2(\tau_0\omega)^\alpha\cos(\alpha\pi/2)+(\tau_0\omega)^{2\alpha}\right]$$
$$-\tfrac{1}{2}\log\left[1+2(\tau_1\omega)^\alpha\cos(\alpha\pi/2)+(\tau_1\omega)^{2\alpha}\right] \tag{8}$$

When the second derivative is taken,

$$\frac{\mathrm{d}^2\log E(\omega)}{(\mathrm{d}\log\omega)^2} = \frac{N_0(\omega)D_1(\omega)-N_1(\omega)D_0(\omega)}{D_0(\omega)D_1(\omega)} \tag{9}$$

with

$$N_k(\omega) = 2\alpha^2\left[(\tau_k\omega)^\alpha\cos(\alpha\pi/2)+2(\tau_k\omega)^{2\alpha}+(\tau_k\omega)^{3\alpha}\cos(\alpha\pi/2)\right] \qquad k=0,1 \tag{10}$$

$$D_k(\omega) = \left[1+2(\tau_k\omega)^\alpha\cos(\alpha\pi/2)+(\tau_k\omega)^{2\alpha}\right]^2, \qquad k=0,1 \tag{11}$$

from relation (9), we see that for

$$\omega = 1\Big/\sqrt{\tau_0\tau_1} = \sqrt{\omega_0\omega_1} = \omega_{\mathrm{inf}} \tag{12}$$

we have

$$\frac{\mathrm{d}^2\log E(\omega_{\mathrm{inf}})}{(\mathrm{d}\log\omega)^2} = 0 \tag{13}$$

The frequency ω_{inf} is the abscissa of the inflexion point of the function $E(\omega)$ in bilogarithmic plotting.

2. Loss Factor Function

Let us express the complex modulus as

$$E^*(\omega) = E_r(\omega) + jE_i(\omega) \tag{14}$$

$$E^*(\omega) = E_r(\omega)[1+j\eta(\omega)] \tag{15}$$

where

$$\eta(\omega) = E_i(\omega)/E_r(\omega) \tag{16}$$

is the loss factor.

The complex modulus and the loss factor can be rewritten as

$$E^*(\omega) = E_0\frac{1+(\tau_0\omega)^\alpha\cos(\alpha\pi/2)+j(\tau_0\omega)^\alpha\sin(\alpha\pi/2)}{1+(\tau_1\omega)^\alpha\cos(\alpha\pi/2)+j(\tau_1\omega)^\alpha\sin(\alpha\pi/2)} \tag{17}$$

$$\eta(\omega) = \frac{\left(\tau_0^\alpha-\tau_1^\alpha\right)\omega^\alpha\sin(\alpha\pi/2)}{1+\omega^\alpha\left(\tau_0^\alpha+\tau_1^\alpha\right)\cos(\alpha\pi/2)+(\tau_0\tau_1)^\alpha\omega^{2\alpha}} \tag{18}$$

For the maximum of the loss factor function,

$$\frac{\mathrm{d}\log\eta(\omega)}{\mathrm{d}\log\omega} = \frac{\left(\tau_0^\alpha-\tau_1^\alpha\right)\left[1-(\tau_0\tau_1)^\alpha\omega^{2\alpha}\right]\sin(\alpha\pi/2)}{\left[1+\left(\tau_0^\alpha+\tau_1^\alpha\right)\omega^\alpha\cos(\alpha\pi/2)+(\tau_0\tau_1)^\alpha\omega^{2\alpha}\right]^2} \tag{19}$$

Then

$$\frac{\mathrm{d}\log\eta(\omega_{\mathrm{inf}})}{\mathrm{d}\log\omega} = 0 \tag{20}$$

Thus, the inflexion frequency ω_{inf} of the magnitude function is also the extremum of the loss factor function, that is, the frequency where the loss factor $\eta(\omega)$ is maximum.

For the evaluation of the maximum loss factor $\eta_{\max}$,

$$\eta_{\max} = \eta(\omega_{\mathrm{inf}}) \tag{21}$$

Thus,

$$\eta_{\max} = \frac{(1-\xi^\alpha)tg(\alpha\pi/2)}{1+\xi^\alpha-2\xi^{\alpha/2}/\cos(\alpha\pi/2)} \tag{22}$$

with

$$\xi = \tau_1/\tau_0 = \omega_0/\omega_1 \tag{23}$$

Here ξ can be neglected for a material that has a large transition region (beyond five decades of frequency). In this case, relation (22) yields

$$\eta_{\max} \cong tg(\alpha\pi/2) \tag{24}$$

Thus,

$$\alpha \cong (2/\pi)\operatorname{arc} tg\,\eta_{\max} \tag{25}$$

III. Parameters Identification

In bilogarithmic plotting, the study of the complex modulus, which is a rational fraction, can be deduced from that of a simple polynomial, that is, the study of $\log E(\omega)$ can be deduced from that of $\log|1+(j\tau\omega)^\alpha|$.

A. Fixed Frequency and Cutoff Frequency

Let us study the polynomial function of α order: $h(\omega) = 1+(j\tau\omega)^\alpha$ with $\tau = 1/\omega_c$. The magnitude of $h(\omega)$ is

$$|h(\omega)| = \sqrt{1+2(\tau\omega)^\alpha\cos(\alpha\pi/2)+(\tau\omega)^{2\alpha}} \tag{26}$$

Figure 1a shows a number of curves for different values of the parameter α. The abscissa represents the reduced frequency $\tau\omega$. Analysis of these curves reveals the existence of an empirical value of frequency ω_f called the fixed frequency. This is the frequency for which $\log|1+(j\tau\omega)^\alpha|$ varies in an insignificant manner. We conclude, therefore, that, for the fixed frequency, the value of $\log|h(\omega_f)|$ remains nearly constant, regardless of the value of α, and is approximately equal to 7.19 dB.

The fixed frequency is situated at 6.23 dB from the cutoff frequency ω_c from where all asymptotes originate in bilogarithmic plotting. Note that the curves are mingled with the asymptotes beyond two decades of frequency.

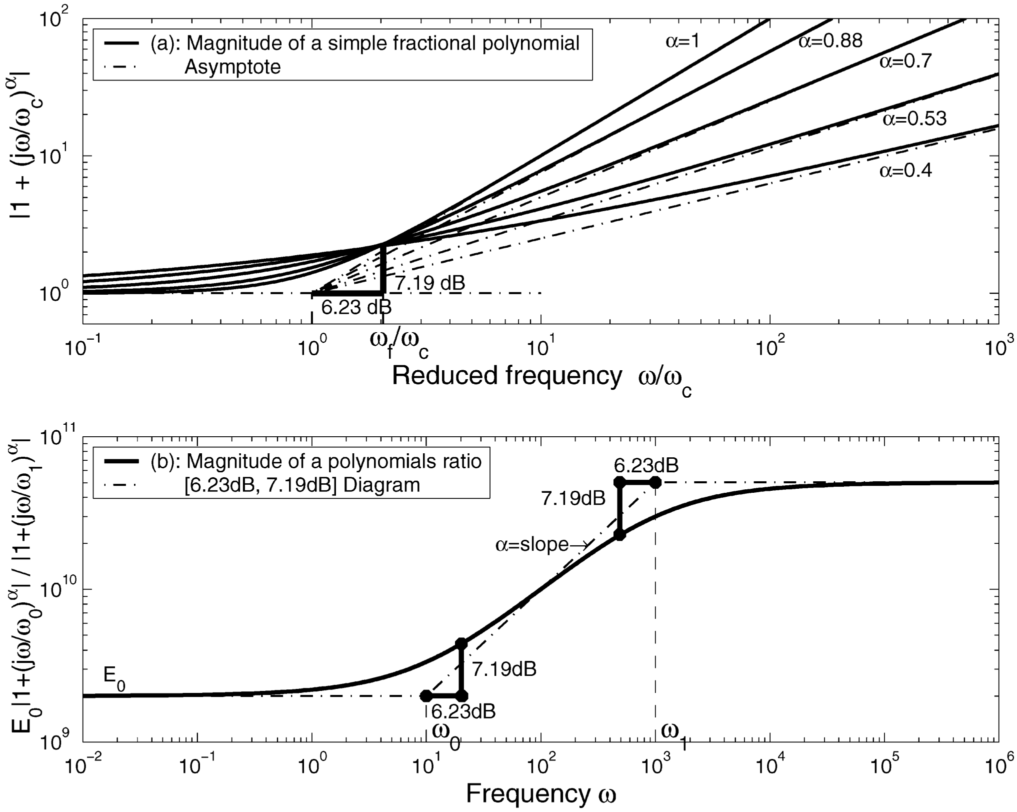

Fig. 1 Cutoff frequency identification.

B. Graphical Method from [6.23 Decibel, 7.19 Decibel]

The method consists in drawing the two horizontal asymptotes and determining on each asymptote the fixed point situated at 7.19 dB from the experimental gain curve (Fig. 1b). The fixed frequencies are the abscissa on the x axis of these two fixed points. The break points are evaluated by displacing -6.23 dB from the first fixed point on the low asymptote and $+6.23$ dB from the second on the top asymptote, respectively. The cutoff frequencies ω_0 and ω_1 are the abscissa of the two break points. The slope of the line connecting the two break points gives the value of the exponent α. The parameter E_0 that corresponds to the static Young's modulus of the material is given by the value of the low asymptote.

Thus, all four characteristic parameters are determined. Consequently, the determination of the function $E^*(\omega)$, which is a complex variable, that is, two real functions, necessitates the knowledge of only one real function, that is, the magnitude $E(\omega)$. The experimental loss factor data could be unknown. The parameters evaluated from magnitude data are used in prediction of the loss factor vs frequency. If the loss factor is known in certain experimental points, it can serve to validate the parameters evaluated.

C. Semigraphical Methods (Derived Methods)

1. *First Technique*

The technique is used when relation (24) is verified. In this case, it is applicable with use of the earlier method. However, it is especially applied when the experimental complex modulus is limited to the sole transition region (no asymptotic part) and the static modulus is known.

The parameter α is given by relation (25). The inflexion frequency is determined from the experimental curve of the loss factor by the maximum $\eta_{\max}$. Its magnitude is given from the gain experimental curve at the frequency ω_{inf} : $E_{\text{inf}} = E(\omega_{\text{inf}})$ (Fig. 2a).

The evaluation of the cutoff frequencies is described next.

By the equation of the segment whose slope defines the exponent parameter, one obtains

$$\log E_0 = \alpha \log \omega_0 + \log \left(E_{\text{inf}} \big/ \omega_{\text{inf}}^{\alpha} \right) \tag{27}$$

The cutoff frequencies are obtained from relations (12) and (27) by

$$\omega_0 = \omega_{\text{inf}} \sqrt[\alpha]{E_0 / E_{\text{inf}}} \tag{28}$$

$$\omega_1 = \omega_{\text{inf}} \sqrt[\alpha]{E_{\text{inf}} / E_0} \tag{29}$$

2. *Second Technique*

This method necessitates the knowledge of the experimental complex modulus on the rubbery plateau (low asymptote) and on the transition region of a material.

The coefficient α is given by Eq. (25). The inflexion frequency ω_{inf} is the abscissa of the point where the loss factor is maximum. The static modulus E_0 is the value of the low asymptote. The cutoff frequency ω_0 is the abscissa of the intersection point of the asymptote and the right gradient α passing through the inflexion point (Fig. 2a). The second cutoff frequency ω_1 is deduced from Eq. (12).

3. *Third Technique*

The cutoff frequency ω_0 is determined by the [6.23 dB, 7.19 dB] method. The maximum loss factor allows the determination of the inflexion frequency ω_{inf} that in turn permits the detection of the inflexion point graphically. The coefficient α is the slope of the line connecting the break point and the inflexion point (Fig. 2a). The static modulus E_0 and the second cutoff frequency ω_1 are determined in the same way as described for the second technical method.

The semigraphical method can be used when the glassy plateau (top asymptote) is known instead of the rubbery one.

D. Higher-Order Fractional Derivative Models (Complex Models)

Sometimes, a viscoelastic material requires a more complicated fractional derivative equation for the relationship of extension deformation, allowing more complicated complex modulus behavior,

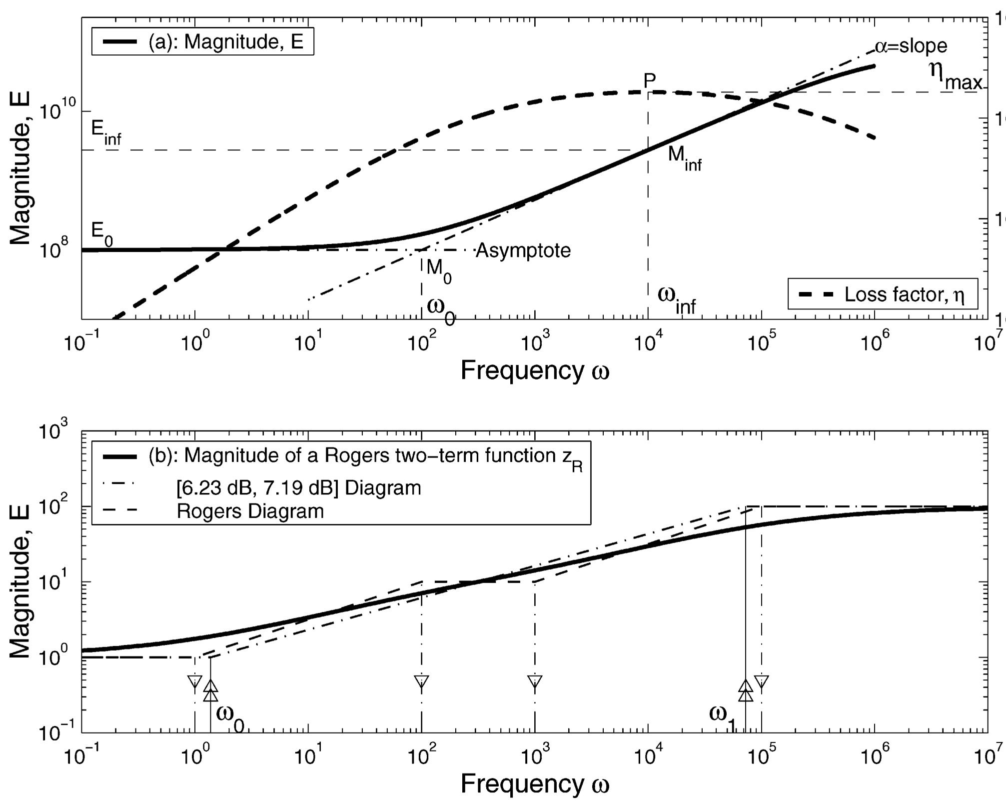

Fig. 2 Derived identification techniques.

which is modeled by Bagley and Torvik[1] as

$$E^*(\omega) = \frac{a + b(j\omega)^\alpha}{1 + c(j\omega)^\beta} \tag{30}$$

where a, b, c, α, and β are real numbers, with $\alpha \neq \beta$. This is theoretically inappropriate.

Jones[6] modeled it by

$$E^*(\omega) = \frac{z_1 + z_2(j\omega)^\alpha}{1 + c(j\omega)^\alpha} \tag{31}$$

where c and α are real numbers and z_1 and z_2 complex numbers.

1. Analysis of Loss Factor Function for Complex Model in Bilogarithmic Plotting

Let us take

$$z_1 = |z_1|e^{j\varphi_1}, \qquad z_2 = |z_2|e^{j\varphi_2} \tag{32}$$

Note that the general form of the complex modulus given by relation (31) introduces a modification on the loss factor behavior, but not on that of the gain.

1) With z_1 and z_2 real numbers, that is, a simple model, the loss factor function tends toward zero at low and high frequencies, with an oblique slope (Fig. 3a). A material example is the 3M-467 adhesive; see Jones's data.[6]

2) With z_1 and z_2 complex numbers, that is, a z_1–z_2 complex model, the loss factor function has horizontal asymptotes whose values are equal to the tangent of the argument of z_1, that is, $\tan\varphi_1$, at low frequencies, and are equal to $\tan\varphi_2$ at high frequencies (Fig. 3d). Material examples include polyisobutylene (PIB) (Nashif et al.),[7] Viton-B, styrene–butadiene–rubber, Soundcoat N5, and Aquaplas F-70 (Antivibe DS).[6]

3) With z_1 a complex number and z_2 a real number, that is, a z_1 complex model, the loss factor function has a horizontal asymptote at low frequencies (equal to $\tan\varphi_1$) and tends toward zero with an oblique slope at high frequencies (Fig. 3b). A material example is butyl rubber.[6]

4) With z_1 a real number and z_2 a complex number, that is, a z_2 complex model, for the loss factor function, there exists a horizontal asymptote at high frequencies (equal to $\tan\varphi_2$), which tends toward zero with an oblique slope at low frequencies (Fig. 3c). An example, material is Corning 10.[1]

2. Identification of Complex Parameters

For complex models, the rationale is first to evaluate the four real parameters E_0, ω_0, ω_1, and α as seen earlier for a simple model. The evaluation of the complex parameters requires the analysis of the loss factor data: The values of the horizontal asymptotes given by the graphical curve of the experimental loss factor in bilogarithmic plotting correspond to $\tan\varphi_1$ at low frequencies and to $\tan\varphi_2$ at high frequencies. Thus, the parameters z_1 and z_2 are given by

$$z_1 = E_0 e^{j\varphi_1}, \qquad z_2 = \left(E_0 \big/ \omega_0^\alpha\right) e^{j\varphi_2} \tag{33}$$

If there does not exist horizontal asymptote at low or/and high frequencies, φ_k is taken null.

IV. Application and Results

A. Simulation

1. [6.23 Decibel, 7.19 Decibel] Method

To model by the [6.23 dB, 7.19 dB] method, we assume a Rogers two-term function z_R given by[3]

$$z_R = \frac{1 + (j\omega/1)^{0.5}}{1 + (j\omega/10^2)^{0.5}} \frac{1 + (j\omega/10^3)^{0.5}}{1 + (j\omega/10^5)^{0.5}}$$

With the help of the [6.23 dB, 7.19 dB] diagram (Fig. 2b), one obtains as an approximating function z_{dB}:

$$z_{\mathrm{dB}} = \frac{1 + (j\omega/1.3763)^{0.424}}{1 + (j\omega/72662)^{0.424}}$$

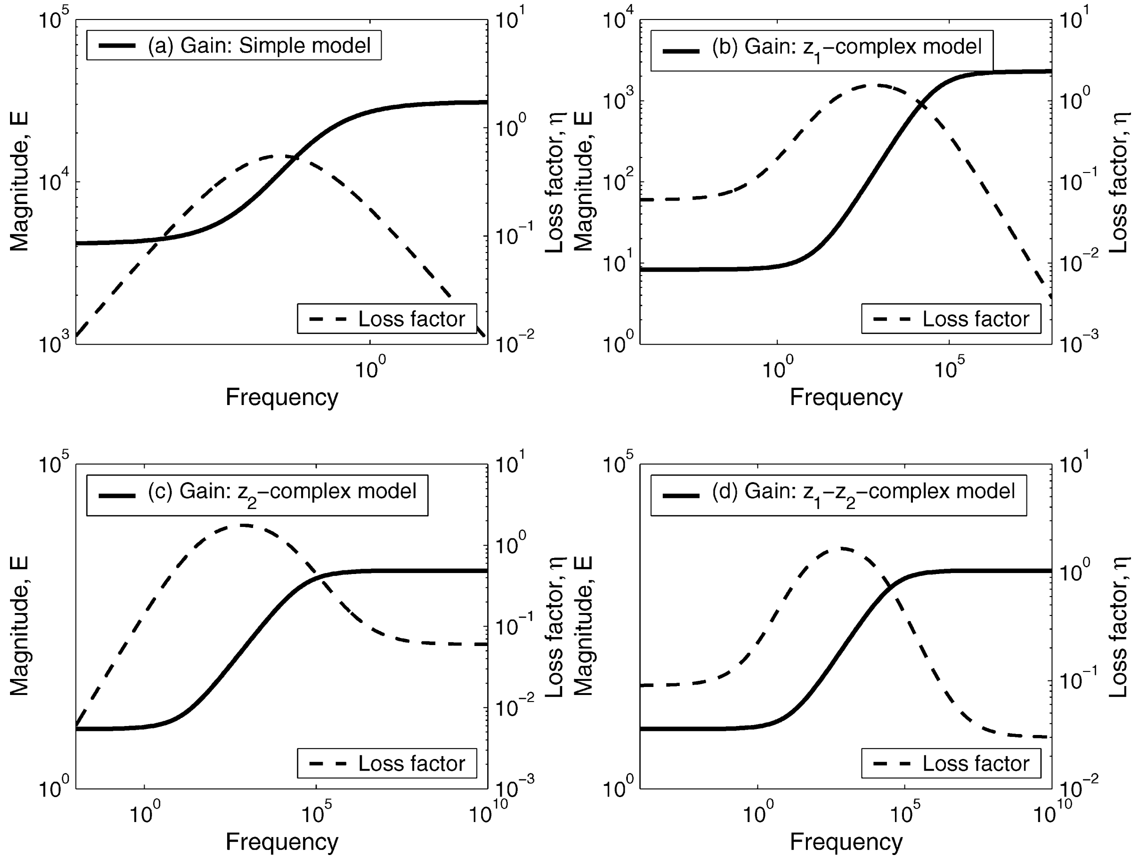

Fig. 3 Fractional models.

2. Semigraphical Method

To identify the parameters of the following function v_e, suppose

$$v_e = \frac{1 + 0.0363(j\omega)^{0.72}}{1 + 1.706110^{-6}(j\omega)^{0.72}}$$

The first technique of the semigraphic method permits us to obtain as approximating function v_n

$$v_n = \frac{1 + 0.0408(j\omega)^{0.711}}{1 + 1.900810^{-6}(j\omega)^{0.711}}$$

B. Experimental Results

1. Corning 10

By use of the proposed [6.23 dB, 7.19 dB] method, one obtains

$$E^*(\omega) =$$

$$4.1510^9 \frac{1 + (0.99986 + j0.016733)(j\omega/0.0063)^{0.67}}{1 + (j\omega/0.1213)^{0.67}} \text{ (N/m}^2\text{)}$$

See Fig. 4a for the comparative curves.

By use of the method of Bagley et al.,[1]

$$E^*(\omega) = \frac{4.1510^9 + 1.0910^{11}(j\omega)^{0.641}}{1 + 3.5(j\omega)^{0.631}} \text{ (N/m}^2\text{)}$$

2. Butyl Rubber

By use of the proposed third semigraphic technique, one obtains

$$E^*(\omega) = 8.2949 \frac{(0.9982 + j0.0599) + (j\omega/12.5992)^{0.6956}}{1 + (j\omega/42210)^{0.6956}} \text{ (MPa)}$$

See Fig. 4b for comparative results.

By the use of the method by Jones,[6]

$$E^*(\omega) = \frac{8.28(1 + j0.06) + 1.38(j\omega)^{0.7}}{1 + 0.0006(j\omega)^{0.7}} \text{ (MPa)}$$

3. PIB

By the use of proposed [6.23 dB, 7.19 dB] method, the complex modulus is

$$E^*(\omega) = 147(0.998 + j0.0632) \frac{1 + (j\omega/40)^{0.666}}{1 + (j\omega/2.510^6)^{0.666}} \text{ (lb/in.}^2\text{)}$$

See Fig. 5a for comparison with the data of Nashif et al.[7]

4. Paracril-BJ with 0 PHR Carbon Black

By use of the proposed [6.23 dB, 7.19 dB] method,

$$E^*(\omega) = 5.238 \left\{ \left[(0.9889 + j0.1483) + (0.9996 + j0.030) \times \left(\frac{j\omega}{13.5998} \right)^{0.6951} \right] \Big/ \left[1 + \left(\frac{j\omega}{86021} \right)^{0.6951} \right] \right\} \text{ (MPa)}$$

See Fig. 5b.

By the use of the method of Jones,[6]

$$E^*(\omega) = \frac{5.18(1 + j0.15) + 0.718(1 + j0.027)(j\omega)^{0.7}}{1 + 0.00035(j\omega)^{0.7}} \text{ (MPa)}$$

Figures 4 and 5 show the predicted (theoretical) curves compared to experimental data of complex modulus. A good overall fit to the experimental magnitude data is sought in the entire range of frequencies. The loss factor prediction also shows a good agreement with experimental data. These results illustrate and confirm the effective use of the fractional model in capturing the precise shape of the complex modulus vs frequency.

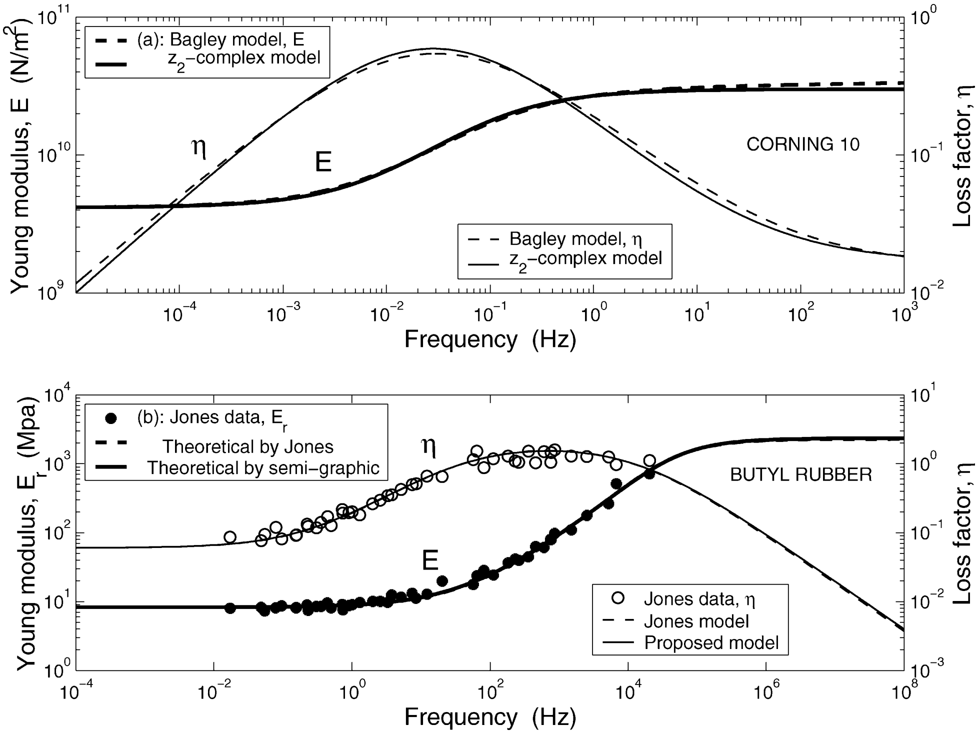

Fig. 4 Results: a) z_2 model and b) z_1 model.

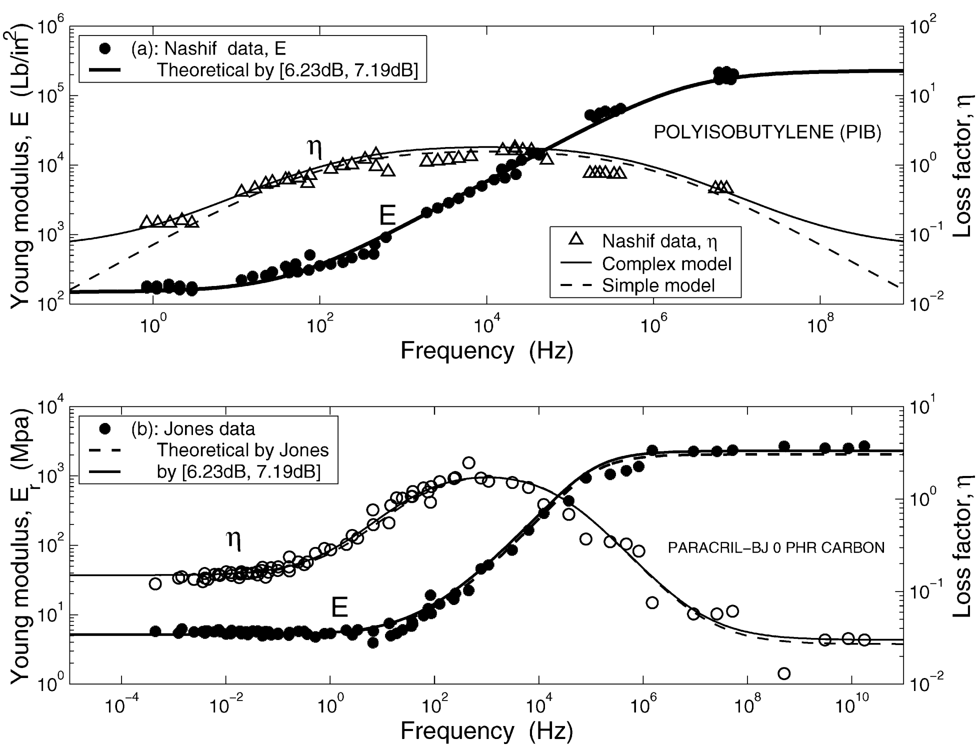

Fig. 5 Model results z_1–z_2.

V. Conclusions

The [6.23 dB, 7.19 dB] technique (Tibi diagram) constitutes an original method that permits the identification of the complex fractional modulus of viscoelastic materials by a graphical or semigraphical approach. The parameters characterizing the viscoelastic behavior can be real or complex numbers, that is, simple and complex materials can be characterized.

In certain cases, the modulus data required to apply the semigraphical method remain limited to the sole transition region of a material. This mitigates difficulties inherent in covering a large range of frequencies experimentally or through the reduced frequency procedure.

The use of the [6.23 dB, 7.19 dB] technique and the derived methods is simple. It requires neither a great deal of experience nor a good mastery of numerical analysis for the user to solve problems, as is usually required in nonlinear identification procedures.

References

[1]Bagley, R. L., and Torvik, P. J., "Fractional Calculus: A Different Approach to the Analysis of Viscoelastic Damped Structures," *AIAA Journal*, Vol. 21, No. 5, 1983, pp. 741–748.

[2]Koeller, R. C., “Application of Fractional Calculus to the Theory of Viscoelasticity,” *Journal of Applied Mechanics*, Vol. 51, 1984, pp. 299–307.

[3]Rogers, L., “An Accurate Temperature Shift Function and a New Approach to Modeling Complex Modulus,” 60th Shock and Vibration Symposium, Virginia Beach, VA, Nov. 1989.

[4]Soula,M., Vinh, T., and Chevaller, Y., “Transient Responses of Polymers and Elastomers Deduced from Harmonic Responses,” *Journal of Sound and Vibration*, Vol. 205, No. 2, 1997, pp. 185–203.

[5]“Electrical and Computer Engineering, Lecture Slides and Notes, Bode Plots,” ECE 222, Portland State Univ., rev., Portland, OR, 2003, http://www.ece.pdx.edu/∼ece2xx/ECE222/Slides/BodePlotsx4.pdf [cited 3 Feb. 2003].

[6]Jones, D. I. G., *Handbook of Viscoelastic Vibration Damping*, Wiley, New York, 2001, Chaps. 2, 5, and 6.

[7]Nashif, A. D., Jones, D. I. G., and Henderson, J. P., *Vibration Damping*, Wiley, New York, 1985, p. 395.

E. Livne
Associate Editor